Journal of Inorganic Biochemistry 175 (2017) 29–35

Contents lists available at ScienceDirect

Journal of Inorganic Biochemistry

journal homepage: www.elsevier.com/locate/jinorgbio

Synthesis and characterization of oxidovanadium complexes as enzyme inhibitors targeting dipeptidyl peptidase IV

Ming-jin Xie[a,*], Ming-rong Zhu[a], Chun-Mei Lu[a], Yi Jin[a], Li-Hui Gao[b], Ling Li[b], Jie Zhou[a], Fan-fang Li[a], Qi Hua Zhao[a], Hong-Ke Liu[c], Peter J. Sadler[d,*], Carlos Sanchez-Cano[d,*]

[a] School of Chemical Science and Technology, Yunnan University, Kunming 650091, Yunnan, China
[b] Biomedical Engineering Research Center, Kunming Medical University, Kunming 650500, Yunnan, China
[c] Jiangsu Collaborative Innovation Center of Biomedical Functional Materials, School of Chemistry and Materials Science, Nanjing Normal University, Wenyuan Road 1, Nanjing 210023, China
[d] Department of Chemistry, University of Warwick, Gibbet Hill Road, Coventry CV4 7AL, UK

ARTICLE INFO

Keywords:
Oxidovanadium (IV)
Schiff base complexes
Enzyme inhibitors
Dipeptidyl peptidase IV
Molecular docking

ABSTRACT

Two oxidovanadium(IV) complexes carrying Schiff base ligands obtained from the condensation of 4,5-dichlorobenzene-1,2-diamine and salicylaldehyde derivatives were synthesised and characterised, including their X-ray crystallographic structures. They were evaluated as dipeptidyl peptidase IV (DPP-IV) inhibitors for the treatment of type 2 diabetes. These compounds were moderate inhibitors of DPP-IV, with IC_{50} values of *ca.* 40 μM. *In vivo* tests showed that complexes **1** and **2** could lower significantly the level of glucose in the blood of alloxan-diabetic mice at doses of 22.5 mg V·kg^{-1} and 29.6 mg V·kg^{-1}, respectively. Moreover, molecular modeling studies suggested that the oxidovanadium complexes **1** and **2** could fit well into the active-site cleft of the kinase domain of DPP-IV. To the best of our knowledge, this is the first report of vanadium complexes capable of inhibiting DPP-IV.

1. Introduction

Type 2 diabetes is a metabolic disease characterised by insulin resistance, hyperglycemia and hyperlipidemia. Dipeptidyl peptidase IV (DPP-IV) inhibitors are a new type of oral hypoglycemic agents for the treatment of patients with type 2 diabetes [1]. Inhibition of the enzyme DPP-IV results in decreased degradation of both glucagon-like peptide-1 (GLP-1) and glucose-dependent insulinotropic peptide (GIP)·Through action *via* GLP-1 and GIP, DPP-IV inhibitors can enhance insulin secretion, control the level of glucose in blood and protect the function of β-cells [2,3]. Consequently, inhibition of DPP-IV is rapidly emerging as a novel therapeutic approach for the treatment of type 2 diabetes, and potent DPP-IV inhibitors have recently been reported [4–7]. A number of X-ray structures of co-crystals of inhibitors and the DPP-IV enzyme have been reported, providing important structural information [8–11].

Vanadium compounds have long been recognised as phosphatase inhibitors, since vanadates are structurally similar to phosphates [12]. Numerous studies have demonstrated that vanadium compounds have insulin-enhancing effects and can improve the symptoms of diabetes in a variety of animal models [13–17]. Vanadyl sulfate and sodium metavanadate have been used in studies with human diabetic patients resembling phase II clinical trials [18–24]. These compounds showed moderate success in alleviating some of the symptoms of diabetes. Due to their wide availability as nutritional supplements they did not go through Phase I clinical trials. Additionally, the chelated complex bis (ethylmaltolato)oxidovanadium(IV) (BEOV) completed Phase I trials and a Phase IIa trial. Clinical trials were discontinued following further pre-clinical safety testing, in which it became clear that renal complications could be precipitated without any obvious warning signs, at slightly higher concentrations than were tried in human volunteers [25–27]. It has been reported that vanadium compounds exert insulin-enhancement effects and cell protection *via* a multiple mechanism involving inhibition of protein-tyrosine phosphatase 1B (PTP1B), activation of peroxisome proliferator-activated receptor (PPARs) – AMP-activated protein kinase (AMPK) signaling, and regulation of unfolded protein responses (UPRs) [28]. Vanadium complexes carrying

Abbreviations: DPP-IV, dipeptidyl peptidase IV; mg V·kg^{-1}, mg Vanadium injected/weight of mice in kg; GLP-1, glucagon-like peptide-1; GIP, glucose-dependent insulinotropic peptide; BEOV, bis(ethylmaltolato)oxovanadium(IV); PTP1B, protein tyrosine phosphatase 1B; PPARs, peroxisome proliferator-activated receptor; AMPK, AMP-activated protein kinase; hIAPP, human islet amyloid polypeptide; DMSO, dimethyl sulfoxide; acac, acetylacetonate; acen, *N,N*-ethylenebis(acetylacetoneiminate); EPR, electron paramagnetic resonance; DMEM, Dulbecco's Modified Eagle's Medium; IC_{50}, 50% inhibition concentration

* Corresponding authors.
E-mail addresses: mjxie@ynu.edu.cn (M.-j. Xie), p.j.sadler@warwick.ac.uk (P.J. Sadler), c.sanchez@warwick.ac.uk (C. Sanchez-Cano).

http://dx.doi.org/10.1016/j.jinorgbio.2017.06.014
Received 14 November 2016; Received in revised form 22 June 2017; Accepted 23 June 2017
Available online 29 June 2017

tridentate Schiff base ligands selectively inhibit PTP1B, and oxidovanadium compounds carrying mixed ligands are highly potent (nanomolar activity) competitive inhibitors for PTP1B [29–31]. Additionally, vanadium complexes have also been shown to inhibit human islet amyloid polypeptide (hIAPP) aggregation [32]. However, the mechanism of action of vanadium complexes ultimately leading to the observed insulin-sensitizing effects is not well understood [33–35]. Therefore, studying their role as enzyme inhibitors and their influence on glucose metabolism is of fundamental importance.

There appear to be no reports exploring the possible role of vanadium or other antidiabetic metal complexes as DPP-IV inhibitors. In this paper, we report two novel oxidovanadium complexes carrying Schiff base ligands obtained from the condensation of 4,5-dichlorobenzene-1,2-diamine and 4-R-salicylaldehyde (where R_1 = H or diethylamine) that have been designed and synthesised as potential DPP-IV enzyme inhibitors. Their biological activity has been assessed by blood glucose-lowering assays, and their interaction with DPP-IV explored by biochemical assays using recombinant DPP-IV and molecular modeling.

2. Experimental

2.1. Materials and methods

All reagents and solvents were purchased commercially as reagent grade and used without further purification unless otherwise stated. Double-distilled water was used to prepare buffer solutions. Vanadyl sulfate hydrate was purchased from the Sigma-Aldrich Chemical Co., and EPR tubes from Wilmad Labglass.

2.2. Preparation of oxidovanadium complexes

The synthetic routes are shown in Scheme 1.

2.2.1. Preparation of [(1E,1′E)-N,N′-(4,5-dichloro-1,2-phenylene)- bis(1-(2-(λ^1-oxidanyl)phenyl)methanimine)] oxidovanadium (IV) (1)

Salicylaldehyde (0.94 g, 5 mmol) dissolved in ethanol was added dropwise to 4,5-dichloride-1,2-phenylenediamine (3 mmol, 0.51 g) in ethanol at room temperature. The mixture was gradually heated to 333 K and maintained at this temperature for 4 h. Then $VOSO_4{\cdot}5H_2O$ (1 mmol, 0.254 g) was added to this solution. The mixture was stirred for about 30 min. The green precipitate was collected and dissolved in dimethyl sulfoxide (DMSO)/dichloromethane (2:1 v/v). Crystals suitable for X-ray diffraction were obtained by slow diffusion of ether into DMSO/dichloromethane (2:1 v/v) solution of the product at 277 K. Yield: 56.5%.

Anal. Calcd. for $C_{20}H_{12}Cl_2N_2O_3V$: %C, 53.3; %H, 2.7; %N, 6.2. Found: %C, 53.6; %H, 2.4; %N, 6.6. UV–vis (DMSO) λ_{max} = 310 nm (ε = 14,847 L·mol^{-1}·cm^{-1}), 325 nm (ε = 17,844 L·mol^{-1}·cm^{-1}), 340 nm (ε = 18,204 L·mol^{-1}·cm^{-1}), 370 nm (ε = 5707 L·mol^{-1}·cm^{-1}), 415 nm (ε = 3868 L·mol^{-1}·cm^{-1}). IR (KBr disk): ν (cm^{-1}) = 1601 ($\nu_{c=N}$), 965 ($\nu_{v=o}$), 598 (ν_{v-o}).

2.2.2. Preparation of [4,4′-((1E,1′E)-((4,5-dichloro-1,2-phenylene)bis(azanylylidene))- bis(methanylylidene))bis(N,N-diethyl-3-(λ^1-oxidanyl)aniline)]-oxidovanadium(IV) DMSO (2)

4-(Diethylamino)salicylaldehyde (9 mmol, 1.85 g) dissolved in ethanol (15 mL) was added dropwise to 4,5-dichloride-1,2-phenylenediamine(3 mmol, 0.51 g) in ethanol (30 mL) at room temperature. The mixture was gradually heated to 333 K and maintained at this temperature for 4 h. Then $VOSO_4{\cdot}5H_2O$ (1 mmol, 0.254 g) was added into this solution. The mixture was stirred for about 30 min. The green-yellow precipitate was collected and dissolved as before. Crystals suitable for X-ray diffraction were obtained by slow diffusion of ether into a DMSO solution of the product at 277 K. Yield: 45.4%.

Anal. Calcd. for $C_{28}H_{30}Cl_2N_4VO_3{\cdot}$DMSO: %C 53.7, %H 5.4, %N 8.4. Found: %C, 53.3; %H, 5.5; %N, 8.6. UV–vis (DMSO) λ_{max} = 376 nm (ε = 4104 L·mol^{-1}·cm^{-1}), 396 nm (ε = 5363 L·mol^{-1}·cm^{-1}), 448 nm (ε = 7793 L·mol^{-1}·cm^{-1}). IR (KBr disk): ν (cm^{-1}) = 1655 ($\nu_{c=N}$), 978 ($\nu_{v=o}$), 567 (ν_{v-o}).

2.3. X-ray crystallography

X-ray diffraction data for complexes **1** and **2** were collected at 298 K using a Bruker Smart Apex II CCD detector with graphite monochromator (ω scan, 2θ max = 56.46) Mo Ka radiation. For complex **1**, a total of 12,051 reflections were collected, with 4252 reflections being unique. For complex **2**, a total of 17,511 reflections were collected, with 5573 reflections being unique. The crystal structures of **1** and **2** were solved by direct method SHLXS-97 (Sheldrick, 1990) and expanded using difference Fourier technique, refined by the program SHLXL-97 (Sheldrick, 1997) and the full-matrix least-squares calculations. The crystal data and structure refinements are given in Table 1.

2.4. IR spectroscopy

Infrared spectra were recorded as KBr pellets in the range 4000–400 cm^{-1} on a Perkin-Elmer Paragon 1000 Fourier-transform spectrometer.

2.5. EPR spectroscopy

EPR spectra were recorded at ambient temperature on a Bruker EMX (X-band) spectrometer. Liquid samples were contained in quartz capillary (I.D. 1.0 mm; O.D. 1.2 mm; Wilmad Labglass) sealed with T-Blu Tac®, placed inside larger quartz tubes (O.D. 2.0 mm) to achieve easy and accurate positioning of the sample inside the resonator. Measurements were made on DMF solutions or on powders at 300 K. Data were fitted using the Easyspin version 5.1.9 software [36].

2.6. DPP-IV inhibition assay

Recombinant DPP-IV was mixed with different concentrations of complexes **1** or **2** (45–0.6 μM) in the assay buffer (100 mM Tris-HCl, 150 mM NaCl, 1.0 mg/mL BSA, pH 8.2). The enzyme reaction was started by addition of a glycyl-L-proline-*p*-nitroanilide tosylate solution and the change in absorbance at 405 nm was monitored for 30 min using a microplate reader (Rayto, Rt-6100, China) [37]. Inhibition constants (IC_{50}) were calculated by fitting the dose-dependent inhibition curves based on the means of several replicate experiments.

2.7. Molecular modeling

To investigate the binding mode of vanadium complexes **1** and **2** to the DPP-IV, the advanced docking program Autodock 3.0.3 was used to dock automatically the inhibitor to the kinase domain of the enzyme. The crystal structure of the kinase domain of DPP-IV in a complex with its inhibitor W61 (PDB entry code 3VJM) was recovered from Brookhaven Protein Database (PDB). The missing atoms and residues were modeled in Sybyl 6.8.17. Atomic charges were taken as Kollman-united-atom [38] for the macromolecule and Gasteiger–Marsili [39] for the inhibitor. To explore the binding mode of compounds to the kinase domain of DPP-IV, the advanced docking program Autodock 3.0.3 [40] was used to dock automatically the inhibitor to the kinase domain of the enzyme. The Lamarckian genetic algorithm (LGA) was applied to analyze inhibitor–enzyme interactions. A Solis and Wets local search performed the energy minimization on a user-specified proportion of the population. The docked conformations of the inhibitor were generated after a reasonable number of evaluations. The whole docking operation in this study can be summarised as follows. First, the kinase domain of DPP-IV was checked for polar hydrogens and assigned for partial atomic charges, then a PDBQ file was created, and the atomic solvation parameters were assigned for the macromolecule. Meanwhile,

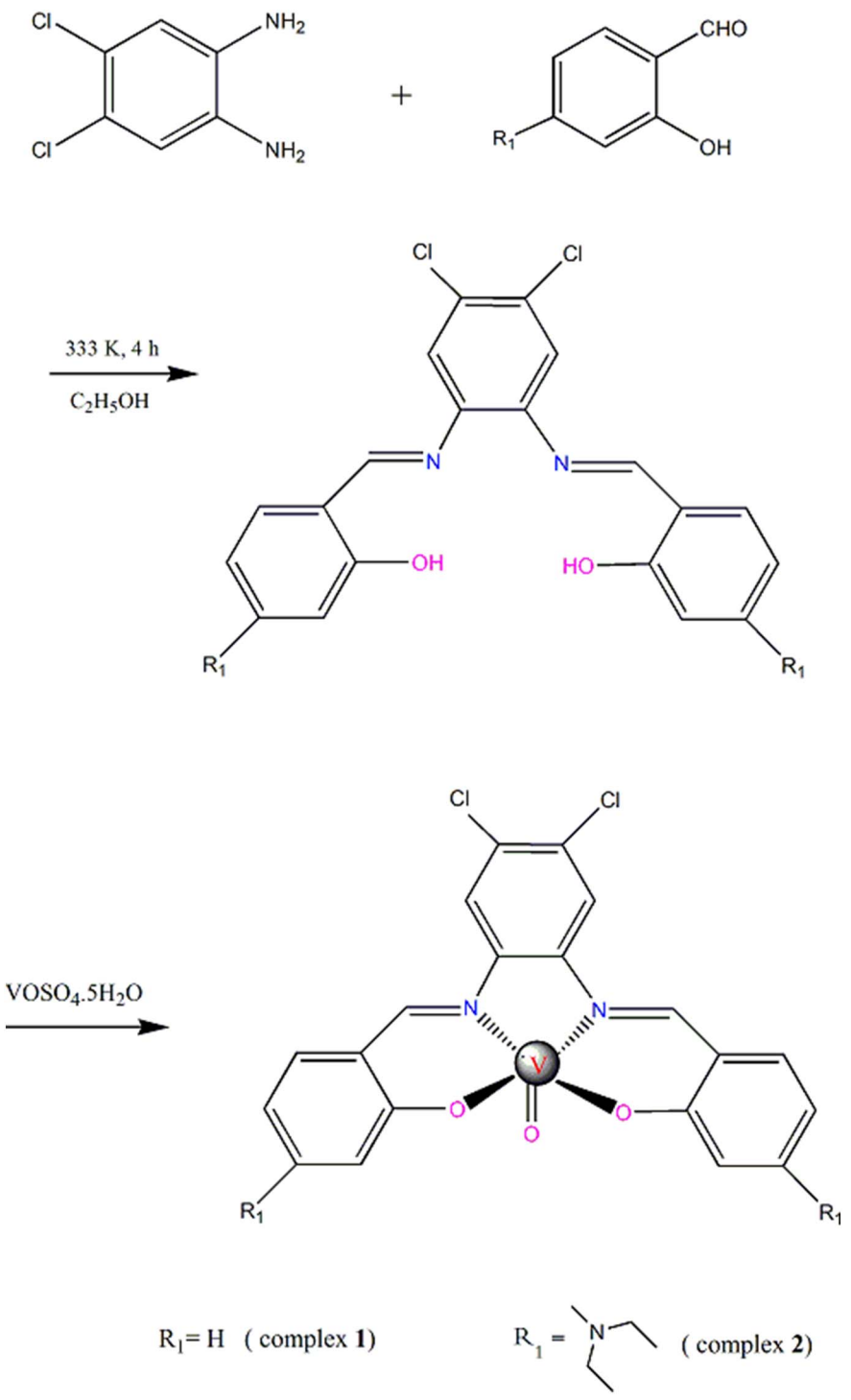

Scheme 1. Synthesis of oxidovanadium complexes **1** and **2.**

some of the torsion angles of the inhibitor that would be explored during molecular docking stage were defined, allowing the conformation search for the ligand during the docking process. Second, the grid map with 60 × 60 × 60 points and a spacing of 0.375 Å was calculated using the AutoGrid program in order to evaluate the binding energies between the inhibitor and the macromolecule. Third, some important parameters for LGA calculations were reasonably set (see Box 1), not only the atom types, but also the generations and the number of runs for the LGA algorithm were edited and properly assigned according to the requirements of the Amber force field. The maximum number of generations, energy evaluations and docking runs were set to 3.0×10^5, 1.5×10^7, and 30, respectively. Finally, the docked complex of the inhibitor–enzyme for the inhibitor was selected according to the criterion of interaction energy combined with geometrical matching quality.

Additionally, to identify the binding sites in DPP-IV, the grid size was set to 100 × 100 × 100 points along the X-, Y-, and *Z*-axes with a 0.375 Å grid spacing. Docking simulations were performed using the Lamarckian genetic algorithm (LGA) and the Solis and Wets local search method. Each run of the docking operation was terminated after a maximum of 2,500,000 energy evaluations.

Table 1
Crystallographic data for complexes **1** and **2**.

Compound	1	2
Empirical	$C_{20}H_{12}Cl_2N_2O_3V$	$C_{28}H_{32}Cl_2N_4O_6SV$
Formula weight	450.16	674.48
Temperature (K)	298(2)	298(2)
Wavelength (Å)	0.71073	0.71073
Crystal size (mm)	0.26 × 0.19 × 0.12	0.28 × 0.21 × 0.14
Space group	*P2(1)/n*	*P2(1)/n*
Crystal system	Monoclinic	Monoclinic
a (Å)	10.4674(11)	16.4371(16)
b (Å)	9.1811(10)	10.1372(10)
c (Å)	18.9133(19)	19.0776(18)
α (°)	90	90
β (°)	95.6180(10)	92.5380(10)
γ (°)	90	90
Volume ($Å^3$)	1808.9(3)	3175.7(5)
Z	4	4
Dcalc (Mg/cm^3)	1.653	1.411
Absorption coefficient (mm^{-1})	1.372	0.592
F(000)	908	1396
Limiting indices	$-10 \le h \le 13$, $-11 \le k \le 12$, $-25 \le l \le 24$	$-17 \le h \le 19$, $-12 \le k \le 12$, $-22 \le l \le 22$
Reflections collected/ unique	12,051/4252[*R*(int) = 0.0369]	17,511/5573[*R*(int) = 0.0379]
Completeness to theta = 25.15	94.40%	100.00%
Refinement method	Full-matrix least-squares on F^{2}	Full-matrix least-squares on F^2
Absorption correction	None	None
Data/restraints/ parameters	4252/0/253	5573/0/385
Goodness-of-fit on F^2	1.01	1.045
Final R indices [$I > 2\sigma(I)$]	R1 = 0.0399, w*R*2 = 0.0957	R1 = 0.0539, w*R*2 = 0.1485
R indices (all data)	R1 = 0.0660, w*R*2 = 0.1090	R1 = 0.0763, w*R*2 = 0.1628
Largest diff. peak and hole(e. Å)	0.307 and −0.306	0.589 and −0.698

2.8. Glucose modulation studies

Male ICR mice weighting 25–30 g were obtained from Chengdu Dossy Experimental Animals Co. Ltd. Sichuan, China. Mice were allowed free access to standard solid food for laboratory animals and tap water. Diabetic mice were generated by a single intraperitoneal injection of alloxan 65 $mg{\cdot}kg^{-1}$ in 0.9% saline. Alloxan is known to induce diabetes in treated animals by destroying pancreatic β-cells through the generation of reactive oxygen species [41]. Therefore, it can be used as an animal model for type 1 diabetes, but also for advanced stages of type 2 diabetes. Four days after alloxan injection, blood samples for analysis of blood glucose were obtained from the tail vein of the mice and the blood glucose were measured by the glucose oxidase method. The alloxan-mice with the blood glucose levels ≧ 11.1 mM were considered as diabetic. Normal mice were injected with 0.9% saline alone.

The experimental animals were randomly divided into four groups with ten mice each. Diabetic control group: alloxan-diabetic mice treated with 0.9% saline; positive groups: alloxan-diabetic mice treated with 250 $mg{\cdot}kg^{-1}$ metformin; treated diabetic group: alloxan-diabetic mice treated with complex **1** 22.5 mg $V{\cdot}kg^{-1}$ (intragastric administration; ig) and **2** 29.6 mg $V{\cdot}kg^{-1}$ (ig) dissolved in 0.5% sodium carboxymethyl cellulose (CMC-Na). The substances above were administered intragastricly once a day at the volume of 10 $mL{\cdot}kg^{-1}$ for 3 weeks. Once per week the blood samples were collected from the tail vein of the mice for the blood glucose assay.

Statistics values were presented as means ± standard deviations. Statistical analysis was performed by one-way analysis of variance followed by Dunnett's multiple comparison tests using Prism version 4.0 software.

Box 1
Vina configuration file.

```
receptor = 1iep_receptorH.pdbqt
    ligand = 1iep_ligandH.pdbqt
    center_x = 15.19
    center_y = 53.903
    center_z = 16.917
    size_x = 15.0
    size_y = 17.25
    size_z = 15.0
    out = 1iep_ligandH_out.pdbqt
```

3. Results and discussion

3.1. Synthesis and the X-ray crystal structure

Vanadyl complexes **1** and **2** were synthesised by the routes shown in Scheme 1. The X-ray crystal structures of complexes **1** and **2** (Fig. 1) show that they are structurally similar to related complexes described previously [42,43]. Bond lengths and angles around the vanadium centre are shown in Tables S1 and S2.

Similarly to other VO(salen) compounds [44,45], complexes **1** and **2** are best described as having closely square-pyramidal geometry, because of their τ values of 0.06 and 0.05. The τ parameter measure the distortion of a square-pyramidal structure toward trigonal bipyramidal [46]. The basal square plane of **1** and **2** is constituted by the Schiff base ligand, which acts as a tetradentate ligand through its imine N atoms and its deprotonated phenolate O atoms. Torsional angles show that atoms N(1)/N(2)/O(2)/O(3) are approximately in one plane, with O1 atoms located at the axial positions. The V═O bond length is 1.596(6) Å, which is typical for five-coordinate vanadyl species, and V−O2 and V−O3 bond lengths in **1** and **2** are all between 1.9162(17) and 1.944(2) Å, typical of single bonds. Additionally, the bond angles in the basal plane are smaller than the vertex angles. This is due to the position of the vanadium(IV) center, which lies above the basal plane of the complex (0.6022 Å in **1**, and 0.5901 Å in **2**).

3.2. Infrared spectroscopy

Vanadium complexes **1** and **2** exhibit a sharp band at *ca.* 966 cm^{-1} due to the ν(V═O) mode [47]. The C═N stretching frequencies for the ligands occur at *ca.* 1620 cm^{-1} and are shifted to lower frequencies (1600–1605 cm^{-1}) in the complexes, indicating the coordination of the imine nitrogens to vanadium [48].

3.3. UV–visible spectroscopy

The VO-complexes were only moderately soluble in methanol, but highly soluble in DMSO. The spectra of the ligands show several sharp absorption maxima in the UV region at approximately 390 nm (ligand **1**), and 352 and 400 nm (ligand **2**), assignable to $\pi \rightarrow \pi^*$ and $n \rightarrow \pi^*$ transitions (see Fig. S1). Upon complexation, the $\pi \rightarrow \pi^*$ transitions shifted to longer wavelengths, while the $n \rightarrow \pi^*$ transition merged with an additional broad intense band at approximately 415 (complex **1**) and 438 (complex **2**) due to ligand-to-metal charge transfer from the phenolate oxygen to empty d orbitals of vanadium.

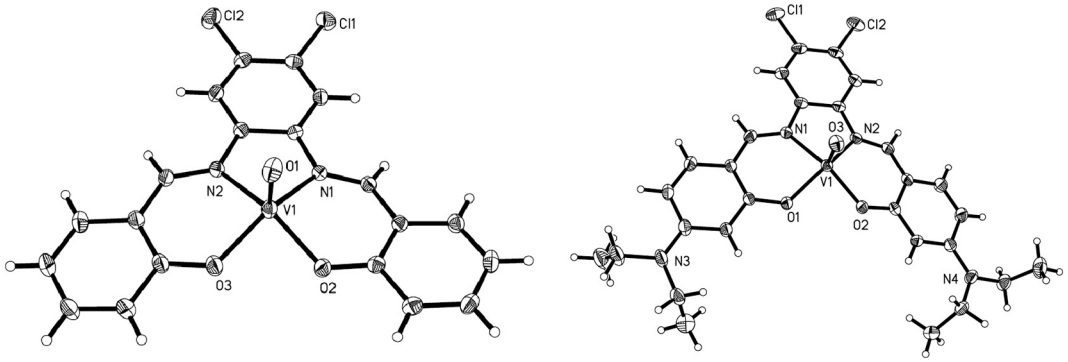

Fig.1. X-ray crystal structures of complexes **1** and **2** with atomic labelling scheme. Displacement ellipsoids are shown at the 30% probability level. The DMSO molecule in **2** has been omitted.

3.4. EPR spectroscopy of VO-complexes

EPR is a useful tool to investigate the nature of the V(IV) centre in oxidovanadium (IV) complexes [49]. The X-band EPR spectra of the complexes were recorded as DMF solutions and powder at 298 K (Fig. S2 and S3). $V^{IV}O$ has a $3d^1$ outer shell configuration and ^{51}V (99.8% abundance) has a nuclear spin quantum number $I = 7/2$ giving rise to the observed hyperfine coupling (8 lines) characteristic of oxidovanadium (IV) complexes [50–52]. Furthermore, g_0 and A_0 values obtained (**1**: $g_0 = 1.972$; $A_0 = 98$ G; **2**: $g_0 = 1.974$; $A_0 = 96.6$ G) are in accordance with the correlation previously established for square-pyramidal vanadyl(IV) complexes with equatorial ligand fields [53].

3.5. DPP-IV inhibition assays by oxidovanadium complexes

DPP-IV is a protein located in the extracellular membrane, but it can also be found in human plasma as a soluble form lacking the transmembrane region [54]. Some of DPP-IV inhibitors are in clinical trials as a new therapy for non-insulin-dependent diabetes mellitus (Type 2 diabetes). The therapeutic benefit is derived from reduced inactivation of incretins GLP-1 and GIP by DPP-IV, thus stimulating greater insulin production, and control the level of glucose in blood in patients with type 2 diabetes [55,56]. Several studies have investigated the efficiency of drugs for the inhibition of DPP-IV [1], but as yet none has involved V compounds.

Both complexes were tested for their ability to inhibit DPP-IV using Gly-Pro-p-nitroanilide as the substrate. The enzyme and complexes were preincubated for 30 min prior to the initiation of the enzymatic reaction by the addition of the substrate. IC_{50} values were obtained by fitting the dose-dependent inhibition curves and was defined as the concentration of the complex needed to reduce the activity of the enzyme by 50%. The IC_{50} values for complexes **1** and **2** are very similar, 38 and 45 μM respectively (Table 2), indicating that the presence of the NEt_2 substituent has little effect on the activity of the complexes. These results indicate moderate inhibition of DPP-IV, although the observed effect is considerably lower than that of clinically-used sitagliptin.

Table 2
IC_{50} values (± SD) for inhibition of DPP-IV by oxidovanadium (IV) complexes.

Compound	IC_{50} (μM)
1	38 ± 2
2	45 ± 3
Sitagliptin[a]	0.018 ± 0.06

[a] Sitagliptin as a positive control was used to evaluate the selected model.

3.6. Molecular modeling study of the interaction of complexes *1*, *2* with DPP-IV

Molecular docking was performed to explore the possible binding of complexes **1** and **2** to the kinase domain of DPP-IV. The blind docking mode with the lowest binding free energy is shown in Figs. 2–3, and S4–S5. The interaction energies between amino residues and complexes **1** and **2** are listed in Tables S3 and S4.

Figs. 2 and S4 show that complex **1** is buried at one end of the active site of the kinase domain of the DPP-IV enzyme. Hydrogen bonds are formed in the active site between the axial oxygen from the oxidovanadium moiety and Asn 710, and one of the hydroxyl groups from the salicylaldimine moieties and Ser 630 residues. Additionally, our model suggests a π-cation interaction between the 4,5-dichloro-1,2-phenylene and nitrogen atoms from the arginine 125 residue, and π–π stacking interaction between the phenyl ring from one salicylaldehyde moiety and the tyrosine 666 residue. Finally, the interaction energies between the enzyme residues and complex **1** indicate that Pro-109, Ile-107 and Lys-463 interact effectively with complex **1** (Fig. 2, and Table S3).

The simulated interaction between complex **2** and the active site of the kinase domain of DPP-IV is shown in Fig. 3 and Fig. S5. Our calculations suggest the presence of hydrogen bonds between the oxygens from both salicylaldimine moieties and the Tyr 547 residue. Additionally, there seem to be π–cation interactions (Arg 669 and 125, respectively) and π–π stacking (Phe 357, His 740 and Tyr 547) between the 4,5-dichloro-1,2-phenylene and one of the salicylaldimine moieties of **2** and the active site of DPP-IV. Interaction energies between the enzyme residues and complex **2** indicate effective interaction with Pro-109, Pro-159 and Ile-107 (Fig. 3 and Table S4).

3.7. Effect of complexes *1* and *2* on blood glucose in alloxan -induced diabetic mice

Complexes **1** and **2** were administered intragastricly to alloxan-diabetic mice for 3 weeks. Metformin was used as positive control. This drug is the only therapeutic agent that has been demonstrated to reduce macrovascular events in type 2 diabetes [57]. The results showed that complex 1 (22.5 mg V·kg^{-1}; 198.8 mg·kg^{-1}) and complex 2 (29.6 mg V·kg^{-1}; 344.1 mg·kg^{-1}) could significantly lower the level of serum glucose in the alloxan-diabetic mice (Fig. 4 and Table S5), when compared with the diabetic control group ($P < 0.05$). After three weeks of treatment, the extent of glucose reduction observed was

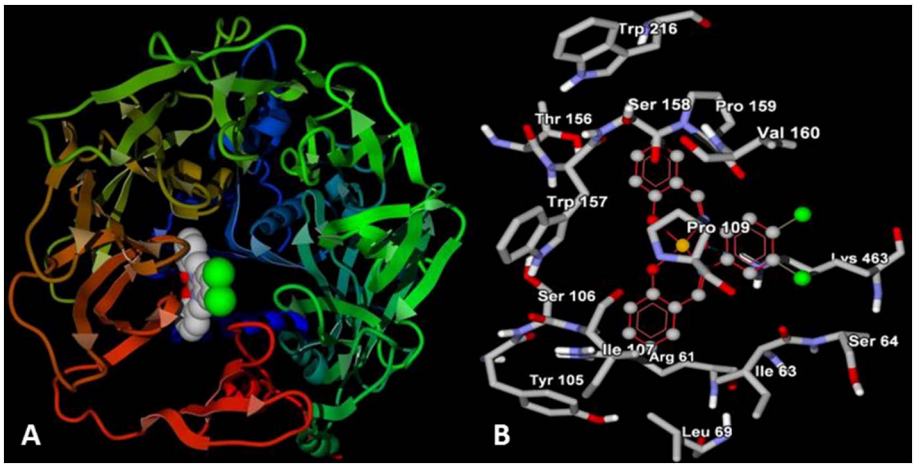

Fig. 2. Docking of **1** in the active site of the kinase domain of DPP-IV. (a) Full view of **1** in DPP-IV with the complex depicted in space-filling representation; (b) detailed illustration of the surroundings near complex **1** in DPP-IV (DPP-IV residues represented as sticks, **1** represented as ball and sticks; O-red, N-blue, Cl-green, V-yellow).

similar to the effect produced by the treatment of mice with metformin (250 mg·kg^{-1}), although none of the compounds administered was able to reduce blood glucose to the levels observed for non-diabetic mice (Table S5). Throughout the experiment, there was no significant difference in body weight among treated and control diabetic mice (Fig. S6). This suggested that **1** and **2** were not toxic at the doses used.

These results are in agreement with evidence previously reported; our compounds show moderate to low activity when compared with similar complexes carrying chlorido substituents on ligands coordinated to V [58–60].

4. Conclusions

Two oxidovanadium (IV) Schiff base complexes with N,N′-1,2-phenylenediamine -bis(salicyladimine) ligands carrying different substituents were synthesised and evaluated as inhibitors of dipeptidyl peptidase IV (DPP-IV) for the treatment of type 2 diabetes. The X-ray structures of complexes **1** and **2** showed that the V(IV) is pentacoordinate and in a distorted square-pyramidal environment. Both complexes significantly inhibit DPP-IV *in vitro*. Molecular modeling shows that complexes **1** and **2** fit well into the active-site cleft of the kinase domain of DPP-IV. Moreover, *in vivo* tests show that **1** (22.5 mg V·kg^{-1}) and **2** (29.6 mg V·kg^{-1}) are as effective in reducing the levels of serum glucose in alloxan-diabetic mice as the clinical drug metformin (250 mg·kg^{-1}). However, oxidovanadium complexes are known to degrade in the gastro-intestinal tract into insoluble and partially soluble vanadate species (which are known phosphatase antagonists that can be used to treat diabetic symptoms). Therefore, further experiments will be needed to determine if **1** and **2** can arrive intact in the plasma of treated mice. Nevertheless, these results constitute the first report of vanadium complexes capable of inhibiting DPP-IV *in vitro*,

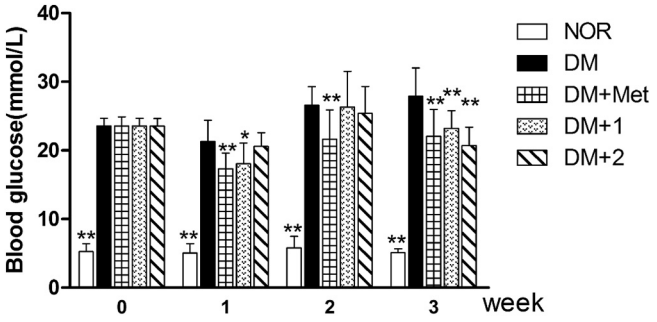

Fig. 4. Effects of intragastric administration of **1** and **2** on blood glucose levels in alloxan-diabetic mice. The diabetic mice (DM) were induced by a single intraperitoneal injection of alloxan 65 mg·kg^{-1}. DM + Met group was treated with metformin at 250 mg·kg^{-1}, DM + 1 group was treated with compound 1 at 22.5 mg V·kg^{-1}, DM + **2** group was treated with compound 2 at 29.6 mg V·kg^{-1}. The normal group (NOR) and DM group were treated with saline. Data are expressed as mean ± standard deviations for 10 mice in each group. $^{*}P < 0.05$ or less *vs* DM group; $^{**}P < 0.01$ or less *vs* DM group (Dunnett's test).

and provide an approach for exploring new design concepts for vanadium agents for incretin-based therapy.

Acknowledgements

We thank the National Natural Science Foundation of China (No. 21161022, 21061016 and 81260502), Yunnan Province (Young and middle-aged academic and technical leaders Program; Grant No. 2001CI002), Key International (Regional) Joint Research Program of NSFC (Grant No. 21420102002), ERC (grant no. 247450) and EPSRC (grant no. EP/F034210/1) for funding.

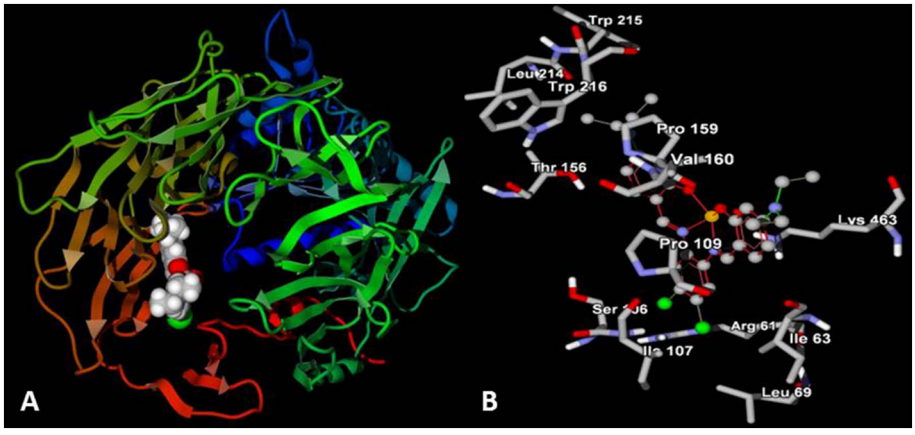

Fig. 3. Docking of complex **2** in the active site of the kinase domain of DPP-IV. (a) Full view of **2** in DPP-IV with the complex depicted in space-filling representation; (b) detailed illustration of the surroundings near complex **2** in DPP-IV (DPP-IV residues represented as sticks, **1** represented as ball and sticks; O-red, N-blue, Cl-green, V-yellow).

Appendix A. Supplementary data

Crystallographic data for **1** and **2** have been deposited in the Cambridge Crystallographic Data Centre (deposition numbers CCDC 1437003 and 1437007, respectively). Copies of these data can be obtained free of charge *via* www.ccdc.cam.ac.uk/conts/retrieving.html (or from the Cambridge Crystallographic Data Centre, 12, Union Road, Cambridge CB21EZ, U.K.; fax: (+ 44) 1223-336-033; or desposit@ccdc.cam.ac.uk). Supplementary data associated with this article can be found in the online version, at http://dx.doi.org/10.1016/j.jinorgbio.2017.06.014.

References

[1] J.-J. Lucienne, J. Med. Chem. 57 (2014) 2197–2212.
[2] G. Abbenante, D.P. Fairlie, Med. Chem. 1 (2005) 71–104.
[3] J.F. Gautier, S. Fetita, E. Sobngwi, C. Salaun-Martin, Diabete Metab. 31 (2005) 233–242.
[4] D.M. Evans, IDrugs 5 (2002) 577–585.
[5] A.E. Weber, J. Med. Chem. 47 (2004) 4135–4141.
[6] C.F. Deacon, Curr. Opin. Investig. Drugs 6 (2005) 419–426.
[7] J.J. Holst, C.F. Deacon, Diabetes 47 (1998) 1663–1670.
[8] M. Yamada, C. Okagaki, T. Higashijima, S. Tanaka, T. Ohnuki, T. Sugita, Bioorg. Med. Chem. Lett. 8 (1998) 1537–1540.
[9] B. Ahren, E. Simonsson, H. Larsson, M. Landin-Olsson, H. Torgeirsson, P. Jansson, M. Sandqvist, P. Båvenholm, S. Efendic, J.W. Eriksson, S. Dickinson, D. Holmes, Diabetes Care 25 (2002) 869–875.
[10] J. Feng, Z. Zhang, M.B. Wallace, J.A. Stafford, S.W. Kaldor, D.B. Kassel, M. Navre, L. Shi, R.J. Skene, T. Asakawa, K. Takeuchi, R. Xu, D.R. Webb, S.L. Gwaltney, J. Med. Chem. 50 (2007) 2297–2300.
[11] R.E. Pratley, Expert. Opin. Pharmacother. 10 (2009) 503–512.
[12] D.C. Crans, J.J. Smee, E. Gaidamauskas, L.Q. Yang, Chem. Rev. 104 (2004) 849–902.
[13] D. Rehder, Inorg. Chem. Commun. 6 (2003) 604–617.
[14] D. Rehder, Met. Ions Life Sci. 13 (2013) 139–169.
[15] Z.L. Gao, C.Y. Zhang, S.W. Yu, X.D. Yang, K. Wang, J. Biol. Inorg. Chem. 16 (2011) 789–798.
[16] Y. Shechter, I. Goldwaser, M. Mironchik, M. Fridkin, D. Gefel, Coord. Chem. Rev. 237 (2003) 3–11.
[17] M. Li, W.J. Ding, B. Baruah, D.C. Crans, J. Inorg. Biochem. 102 (2008) 1846–1853.
[18] D.C. Crans, J. Org. Chem. 80 (2015) 11899–11915.
[19] A.B. Goldfine, D.C. Simonson, F. Folli, M.E. Patti, C.R. Kahn, J. Clin. Endocrinol. Metab. 80 (1995) 3311–3320.
[20] N. Cohen, M. Halberstam, P. Shlimovich, C.J. Chang, H. Shamoon, L. Rossetti, J. Clin. Invest. 95 (1995) 2501–2509.
[21] A.B. Goldfine, M.E. Patti, L. Zuberi, B.J. Goldstein, R. LeBlanc, E.J. Landaker, Z.Y. Jiang, G.R. Willsky, C.R. Kahn, Metabolism 49 (2000) 400–410.
[22] M. Halberstam, N. Cohen, P. Shlimovich, L. Rossetti, H. Shamoon, Diabetes 45 (1996) 659–666.
[23] X. Wang, T. Sun, J. Liu, Z. Shan, Y. Jin, S. Chen, W. Bao, F.B. Hu, L. Liu, Am. J. Epidemiol. 180 (2014) 378–384.
[24] G.R. Willsky, A.B. Goldfine, P.J. Kostyniak, J.H. McNeill, L.Q. Yang, H.R. Khan, D.C. Crans, J. Inorg. Biochem. 85 (2001) 33–42.
[25] K.H. Thompson, C. Orvig, J. Inorg. Biochem. 100 (2006) 1925–1935.
[26] K.H. Thompson, J. Lichter, C. LeBel, M.C. Scaife, J.H. McNeill, C. Orvig, J. Inorg. Biochem. 103 (2009) 554–558.
[27] M.W. Makinen, M. Salehitazangi, Coord. Chem. Rev. 279 (2014) 1–22.
[28] X. Niu, R. Xiao, N. Wang, Z. Wang, Y. Zhang, Q. Xia, X. Yang, Curr. Top. Med. Chem. 16 (2016) 811–822.
[29] C.X. Yuan, L.P. Lu, X.L. Gao, Y.B. Wu, M.L. Guo, Y. Li, X.Q. Fu, M.L. Zhu, J. Biol. Inorg. Chem. 14 (2009) 841–851.
[30] C.X. Yuan, L.P. Lu, Y.B. Wu, Z.W. Liu, M.L. Guo, S. Xing, X.Q. Fu, M.L. Zhu, J. Inorg. Biochem. 104 (2010) 978–986.
[31] L.P. Lu, X.L. Gao, M.L. Zhu, S.L. Wang, Q. Wu, S. Xing, X.Q. Fu, Z.W. Liu, M.L. Guo, Biometals 25 (2012) 599–610.
[32] L. He, X.S. Wang, C. Zhao, D.S. Zhu, W.H. Du, Metallomics 6 (2014) 1087–1096.
[33] K.G. Peters, M.G. Davis, B.W. Howard, M. Pokross, V. Rastogi, C. Diven, K.D. Greis, E. Eby-Wilkens, M. Maier, A. Evdokimov, S. Soper, F. Genbauffe, J. Inorg. Biochem. 96 (2003) 321–330.
[34] G. Huyer, S. Liu, J. Kelly, J. Moffat, P. Payette, B. Kennedy, G. Tsaprailis, M.J. Gresser, C. Ramachandran, J. Biol. Chem. 272 (1997) 843–851.
[35] F. Nxumalo, N.R. Glover, A.S. Tracey, J. Biol. Inorg. Chem. 3 (1998) 534–542.
[36] S. Stoll, A. Schweiger, J. Magn. Reson. 178 (2006) 42–55.
[37] A. Karasik, P. Aschner, H. Katzeff, M.J. Davies, P.P. Stein, Curr. Med. Res. Opin. 24 (2008) 489–496.
[38] S.J. Weiner, P.A. Kollman, D.A. Case, U.C. Singh, C. Ghio, G. Alagona, S. Profeta, P. Weiner, J. Am. Chem. Soc. 106 (1984) 765–784.
[39] J. Gasteiger, M. Marsili, Tetrahedron 36 (1980) 3219–3228.
[40] (a) G.M. Morris, D.S. Goodsell, R.S. Halliday, R. Huey, W.E. Hart, R.K. Belew, A.J. Olson, J. Comput. Chem. 19 (1998) 1639–1662;
(b) G.M. Morris, D.S. Goodsell, R. Huey, W.E. Hart, R.S. Halliday, R.K. Belew, A.J. Olson, AUTODOCK, M. Version 3.0.3. The Scripps Research Institute, Molecular Graphics Laboratory, Department of Molecular Biology, (1999).
[41] S. Lenzen, Diabetologia 51 (2008) 216–226.
[42] X. Wang, X.M. Zhang, H.X. Liu, Polyhedron 14 (1995) 293–296.
[43] M.J. Xie, L. Li, X.D. Yang, W.P. Liu, S.P. Yan, Y.F. Niu, Z.H. Meng, Eur. J. Med. Chem. 45 (2010) 2327–2335.
[44] M. Pasquali, F. Marchetti, C. Floriani, M. Cesari, Inorg. Chem. 19 (1980) 1198–1202.
[45] P.E. Riley, V.L. Pecoraro, C.J. Carrano, J.A. Bonadies, K.N. Raymond, Inorg. Chem. 25 (1986) 154–160.
[46] C.R. Cornman, K.M. Geisre-Bush, S.R. Rowley, P.D. Boyle, Inorg. Chem. 36 (1997) 6401–6408.
[47] S. Mondal, S.P. Rath, K.K. Rajak, A. Chakravorty, Inorg. Chem. 37 (1998) 1713–1719.
[48] A.D. Westland, M.T.H. Tarafder, Inorg. Chem. 20 (1981) 3992–3995.
[49] N. Raman, S.J. Raja, J. Joseph, J.D. Raja, Russ. J. Coord. Chem. 33 (2007) 7–11.
[50] S. Bhattacharya, T. Ghosh, Transit. Met. Chem. 27 (2002) 89–94.
[51] M. Mathieu, P. Van Der Voort, B.M. Weckhuysen, R.R. Rao, G. Catana, R.A. Schoonheydt, E.F. Vansant, J. Phys. Chem. B 105 (2001) 3393–3399.
[52] J.C. Pessoa, I. Cavaco, I. Correia, D. Costa, R.T. Henriques, R.D. Gillard, Inorg. Chim. Acta 305 (2000) 7–13.
[53] J.S. Hwang, M.O. Hamad Al-Turabi, Energy Fuel 14 (2000) 179–183.
[54] A.M. Lambeir, C. Durinx, S. Scharpe, I. De Meester, Crit. Rev. Clin. Lab. Sci. 40 (2003) 209–294.
[55] J.D. Drucker, Expert Opin. Investig. Drugs 12 (2003) 87–100.
[56] A. Weber, J. Med. Chem. 47 (2004) 4135–4141.
[57] I. Brandt, J. Joossens, X. Chen, M.B. Maes, S. Scharpe, I.D. Meester, A.M. Lambeir, Biochem. Pharmacol. 70 (2005) 134–143.
[58] T. Takino, H. Yasui, A. Yoshitake, Y. Hamajima, R. Matsushita, J. Takada, H. Sakurai, J. Biol. Inorg. Chem. 6 (2001) 133–142.
[59] J.J. Smee, J.A. Epps, K. Ooms, S.E. Bolte, T. Polenova, B. Baruah, L. Yang, W. Ding, M. Li, G.R. Willsky, A. Cour, O.P. Anderson, D.C. Crans, J. Inorg. Biochem. 103 (2009) 575–584.
[60] M.J. Xie, Y.F. Niu, X.D. Yang, W.P. Liu, L. Li, L.H. Gao, S.P. Yan, Z.H. Meng, Eur. J. Med. Chem. 45 (2010) 6077–6084.